UNIVERSITYOF BIRMINGHAM

University of Birmingham
Research at Birmingham

Contributing to DSO's Energy-Reserve Pool: A Chance-Constrained Two-Stage µ VPP Bidding Strategy
Fu, Hao; Wu, Zhi; Zhang, Xiao-ping; Brandt, Joachim

Link to publication on Research at Birmingham portal

Contributing to DSO's Energy-Reserve Pool: A Chance-Constrained Two-Stage µVPP Bidding Strategy

HAO FU[1,2], ZHI WU [ID][1,4], XIAO-PING ZHANG [ID][3] (Senior Member, IEEE), AND JOACHIM BRANDT[5]

[1]Department of Electronic, Electrical, and Systems Engineering, University of Birmingham, Birmingham B15 2TT, U.K.
[2]Department of System Planning, Central Southern China Electric Power Design Institute, Wuhan 430071, China
[3]Department of Electronic, Electrical, and Systems Engineering, University of Birmingham, Birmingham B15 2TT, U.K.
[4]School of Electrical Engineering, Southeast University, Nanjing 210096, China
[5]Commercial Energy Management, E.ON, Nottinghamshire NG15 0DR, U.K.
CORRESPONDING AUTHOR: X.-P. ZHANG (x.p.zhang@bham.ac.uk)

ABSTRACT This paper presents the strategic proposition for a micro virtual power plant (**µ** VPP) to participate in the distribution level energy-reserve pool managed by a distribution system operator. A chance-constrained two-stage stochastic formulation is proposed to derive the bidding strategy for **µ** VPP maximizing its daily profit. The stochastic nature of renewable generation and load profile of the **µ** VPP is captured by the Monte Carlo method. The security of supply is guaranteed by controlling the loss of load probability, which is modeled as chance constraint. The numerical tests are performed on **µ** VPPs with different penetration levels of distributed energy resource (DER) and renewable energy source (RES), where the impact of the DER and RES indexes and the impact of uncertainty levels are demonstrated. Also, the advantages of chance-constrained formulation as the means of risk-hedging are addressed. Finally, the impact of rival **µ** VPPs on the bidding behaviors and the impact of carbon taxes on the profit are analyzed.

INDEX TERMS Micro virtual power plant (µ VPP), local energy-reserve pool, distribution system operator (DSO), chance-constrained formulation, carbon tax.

I. INTRODUCTION

THE duel challenges of making the transition to a low carbon economy while securing energy supplies led to a £32 billion plan to rewire Britain over a time span of two decades, announced by the Office of Gas and Electricity Markets (OFGEM) in 2010 [1]. Distributed Energy Resource (DER), despite of its inherent advantages, has also brought negative impacts on electricity networks. The intermittent nature of household renewable generation can potentially compromise system reliability by inflicting balancing challenges in the UK distribution network [2]. However, the negative impacts can be mitigated and DER's potential can be better exploited in an aggregated approach such as Microgrid (MG) and Virtual Power Plant (VPP). A coordinated, distribution level pool should also be established which provides access to the participating MGs and VPPs. The behavior of each participant is worth investigating.

Previous publications have designed a two-stage market consisting of a day-ahead (DA) market and a real-time balancing (RT) market for MG and VPP. MG and VPP are more vulnerable to shortage risks due to volatility in market prices, demand and generation capacity compared with Macrogrid. If they practice as sole electricity market players, the only available hedging method against shortage risk is to purchase from grid at spot prices, which can be quite high at times of peak load [3], [4]. Thus, in [5] and [6] it has been suggested that MG and VPP should contribute reserve capacity to the nearby feeders of distribution network when necessary. Also in [3] it has been pointed out that small-scale MGs/VPPs participating in the distribution level market could be modeled as price-takers.

The bidding behavior of MG/VPP could be modeled as a deterministic linear programming problem [7], [8] with linearized fuel cost for dispatchable generators. To better

address the considerable impact of uncertainties, stochastic models were applied in [9]–[13]. The fluctuations in generation and demand were often assumed to follow a normal distribution and adequate number of scenarios were generated to form the uncertain profile. Although in [9]–[12] the amount of electricity to be purchased from/sold to the utility grid and commitment of DERs that serve their optimization purposes was identified, and there was a lack of concerns for reserve flexibilities. A modified approach was proposed in [13] to assess reserve capacity sourced from DERs. However, the reserve resource in the works above was not contributing to other participants of the reserve pool, thus its opportunity to generate a value stream was denied.

Various optimization techniques were applied to hedge against the risk brought by the uncertainties. In [14]–[16] robust optimization approach was utilized to construct a solution that is deterministically immune for any realization of the uncertainty in a given set. Conditional value at risk was introduced as a risk management scheme in [11] and [12] to control the trade-off between the expected economic profit and the variability caused by uncertain components. Chance-constrained optimization was introduced as a reliable solution to stochastic optimization problems. In the chance-constrained optimization, some constraints can be relaxed with a predefined small level of probability, or must be satisfied with a high level of probability. The early application of this method was found in unit commitment problems which considers uncertain demand and random outages of power system components [17], [18]. In recent years there has been an increasing interest in utilizing chance-constrained optimization due to the rising penetration level of RES [19]–[21] where chance-constrained optimization is utilized in optimal power flow, transmission network operation and unit commitment scheduling. However, to the best of our knowledge, application of chance-constrained optimization in deriving the μVPPs' bidding strategy has not been discussed in the literature yet. Compared with the proposed chance-constrained method, robust optimization can be too conservative with its worst-case-oriented decisions. Although conditional value at risk method is a similar probabilistic risk measure, it only controls the variability indirectly in financial terms. On the other hand, the proposed chance-constrained method interacts directly with the uncertainties in physical systems such as LOLP. LOLP is the likelihood of involuntary load disconnection due to the disruption in power supply.

This paper presents the bidding strategy for a micro Virtual Power Plant (μVPP). μVPP is defined as an extension to the MG concept since the DER located within the μVPP has a capacity that can cover either partial or all of the load demand. The bidding strategy is derived from a chance-constrained two-stage stochastic formulation and the main contributions of this paper are identified as follows:

1. μVPP is established as an active contributor of a distribution level energy-reserve pool.
2. Compared with the classical Monte Carlo recourse method, the proposed chance-constrained formulation

demonstrates its ability to maintain the LOLP at a required level. It takes less processing time yet renders no loss of optimality.
3. The impacts of different levels of forecast error and LOLP on bidding behavior and expected profit are analyzed, which provide insights to μVPP owners with different sizes of DER and RES.
4. The impact of rival μVPP on the bidding behaviors with congestion is analyzed. Also the results demonstrate how μVPP owners will be affected by the implementation of carbon tax.

This paper is organized into five sections. Section II describes the market structure and the business model. Section III presents the two-stage chance-constrained formulation of the bidding strategy. The numerical results are displayed and analyzed in Section IV. Section V draws the conclusion and addresses the key findings.

II. μVPP BUSINESS MODEL IN ENERGY-RESERVE POOL

By pooling the energy and reserve capacities resourced from both local DERs and traditional suppliers, a market is established in the distribution system as shown in Fig. 1. The
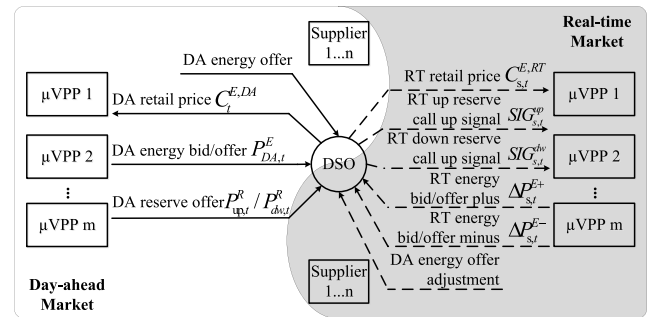
FIGURE 1. Energy-reserve pool in distribution system.

participants in the market including μVPPs and energy suppliers are managed by a Distribution System Operator (DSO). The dual role of μVPP as both producer and consumer enables a submission of either energy offer or energy bid to the market, depending on the capacity of DER and the demand level inside μVPP. The proposed distribution system pool introduces more competition to the retail energy market and provides μVPPs with the liberty to switch between producer and consumer in daily operation.

In DA market, the DA retail energy price $C_t^{E,DA}$ (£/kWh) is broadcasted by the DSO to the market participants. Based on the price signals, μVPPs submit two sets of hourly quantity bid/offer: the energy bid or offer $P_{DA,t}^E$ (kW) to purchase or sell energy and the upward or downward reserve offer $P_{up,t}^R / P_{dw,t}^R$ (kW) to provide regulating service. In the RT market, the retail energy price is updated to $C_{s,t}^{E,RT}$ (£/kWh). Thus, changes are made to the energy bid/offer as the μVPP needs to purchase/sell more energy $\Delta P_{s,t}^{E+}$ (kW) or less $\Delta P_{s,t}^{E-}$ (kW). Should the need arise for the provision of reserve capacity, call up signals $SIG_{s,t}^{up}/SIG_{s,t}^{dw}$ will be issued

by the DSO and the μVPPs that are called up will produce the requested amount of regulating power as they offer in the DA market. To sum up, the DA market matches the electricity demand bids and supply offers from pool participants and the RT market settles the imbalanced power to achieve real-time balance of supply and demand.

To illustrate the context and beneficiaries of the energy-reserve pool in the distribution system, the μVPP business model should be developed addressing the roles and value transactions between players including DSO, μVPP and end-users as presented in Fig. 2.
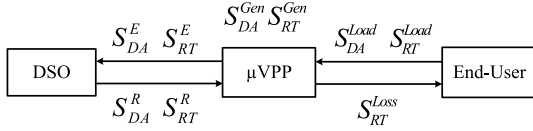

FIGURE 2. Value transactions between distribution system market participants.

1) μVPP-DSO

DSO manages the pool market and channels the value stream between participants from energy and reserve capacity transactions. According to the Common Distribution Charging Methodology [22] issued by OFGEM, a capacity charge determined by the highest kW power flow at the grid connection point will be included in the energy tariff. Thus, DSO charges/pays μVPP for its DA energy bid/offer $P^E_{DA,t}$ (kW) at price $\eta C^{E,DA}_t$ (£/kWh), where the ratio η implies that a higher transaction limit corresponds to more expensive tariff. Also in the DA market, the DSO pays each μVPP for the submission of upward or downward reserve offer $P^R_{up,t}/P^R_{dw,t}$ (kW) at price C^R_{DA} (£/kWh). Later in the RT market, μVPP's payment/income from the DA energy bid/offer could be affected by two sources: the upward or downward changes to the DA energy bid/offer and the difference between the RT energy tariff $C^{E,RT}_{s,t}$ (£/kWh) and the DA energy tariff. Another RT income for the μVPP comes from the provision of reserve capacity at RT reserve price C^R_{RT} (£/kWh). μVPP will receive this income only if its DA reserve offer is called up to produce.

$$
\begin{aligned}
S^{DSO}_{uVPP} &= S^R_{DA} + S^R_{RT} - S^E_{DA} - S^E_{RT} \\
&= C^R_{DA} \sum_{t=1}^{NT} \left(P^R_{up,t} + P^R_{dw,t} \right) \\
&+ C^R_{RT} \pi^*_s \sum_{s=1}^{NS} \sum_{t=1}^{NT} \left(P^R_{up,t} SIG^{up}_{s,t} + P^R_{dw,t} SIG^{dw}_{s,t} \right) \\
&- \sum_{t=1}^{NT} \eta C^{E,DA}_t P^E_{DA,t} \\
&- \pi^*_s \sum_{s=1}^{NS} \sum_{t=1}^{NT} \eta C^{E,RT}_{s,t} \left(\Delta P^{E+}_{s,t} - \Delta P^{E-}_{s,t} \right) \\
&- \pi^*_s \sum_{s=1}^{NS} \sum_{t=1}^{NT} \eta \left(C^{E,RT}_{s,t} - C^{E,DA}_{s,t} \right) P^E_{DA,t} \quad \forall s, \forall t
\end{aligned}
\tag{1}
$$

where the first term of equation represents the revenue of μVPP S^R_{DA} (£) for the provision of reserve offers in the DA market. This income is obtained whether the offers are called up or not. The second term stands for the payment S^R_{RT} (£) in the RT market when the reserve capacity is called up to produce. The third term is the cost S^E_{DA} (£) of purchasing energy or the income of selling energy in the DA market. The last two terms constitute the RT cost/income variation S^E_{RT} (£). In equation (1), the RT value stream S^R_{RT} and S^E_{RT} under each scenario s are assigned with the probability π^*_s.

2) μVPP INHERENT COST

The DER located in the proposed μVPP includes small or medium scale wind turbines and diesel generators. The operation cost of wind turbines is assumed to be zero, leaving the inherent cost to be the operation cost of diesel generators

$$
S^{Gen}_{DA} = \sum_{t=1}^{NT} \sum_{i=1}^{NG} \left(C^{Gen}_i P^{Gen}_{i,t} + C^{SU}_i u_{i,t} + C^{SD}_i v_{i,t} \right) \quad \forall i, \forall t
\tag{2}
$$

where the price parameters include fuel cost C^{Gen}_i (£/kWh) for hourly power output $P^{Gen}_{i,t}$ (kW), start-up cost C^{SU}_i (£) and shut-down cost C^{SD}_i (£). In the RT market, the diesel generators must ramp up or ramp down their output power $\Delta P^{Gen}_{s,i,t}$ (kW) to accommodate the changes in demand level and fulfill the task to produce reserve capacity. The variation of operation cost is therefore calculated as

$$
S^{Gen}_{RT} = \pi^*_s \sum_{s=1}^{NS} \sum_{t=1}^{NT} \sum_{i=1}^{NG} C^{Gen}_i \Delta P^{Gen}_{s,i,t} \quad \forall s, \forall i, \forall t.
\tag{3}
$$

3) μVPP-END-USER

To encourage end-users to join the μVPP community, a discount rate ω is applied for the retail energy price. Based on the DA prediction of load, μVPP estimates a retail income S^{Load}_{DA} (£) from end-users

$$
S^{Load}_{DA} = \sum_{t=1}^{NT} \omega \eta C^{E,DA}_t P^{L,DA}_t \quad \forall t
\tag{4}
$$

where $\omega \eta C^{E,DA}_t$ is the DA energy price with discount for the end-users in the μVPP and $P^{L,DA}_t$ (kW) is the forecasted load.

In the RT market scenarios, both the retail energy price and the actual demand vary from DA forecasted value, the variation of retail income is calculated as

$$
S^{Load}_{RT} = \pi^*_s \sum_{s=1}^{NS} \sum_{t=1}^{NT} \omega \eta C^{E,RT}_{s,t} \left(P^{L,RT}_{s,t} - P^{L,DA}_t \right) \quad \forall s, \forall t
\tag{5}
$$

where $\omega \eta C^{E,RT}_{s,t}$ is the RT energy price and $P^{L,RT}_{s,t}$ (kW) is the RT load level in each scenario. Additionally, a small level of load loss $P^{loss}_{s,t}$ (kW) is tolerable in the μVPP supply commitment but the end-users should be well compensated

at the penalty price C_{loss} (£/kWh)

$$S_{RT}^{Loss} = \pi_s^* \sum_{s=1}^{NS} \sum_{t=1}^{NT} C_{loss} P_{s,t}^{loss} \quad \forall s, \forall t. \tag{6}$$

III. CHANCE-CONSTRAINED TWO-STAGE STOCHASTIC μVPP BIDDING STRATEGY FORMULATION

The uncertain components in the μVPP include wind power output, load level, RT energy price and RT call up signals for reserve offers. A truncated normal distribution is used to mimic the DA forecast error of the first three components [23].

$$P_{s,t}^{W,RT} \sim TN(P_t^{W,DA}, \sigma_W^2) \quad \forall s, \forall t \tag{7}$$

$$P_{s,t}^{L,RT} \sim TN(P_t^{L,DA}, \sigma_L^2) \quad \forall s, \forall t \tag{8}$$

$$C_{s,t}^{E,RT} \sim TN(C_t^{E,DA}, \sigma_{CE}^2) \quad \forall s, \forall t \tag{9}$$

where the DA forecasted values $P_t^{W,DA}$, $P_t^{L,DA}$ and $C_t^{E,DA}$ are used as the mean value in equation (7)-(9) and the forecast error is represented by the standard deviation of each component. As for the RT call up signals for reserve offers, they are generated as random binary signals with a low probability of signal "1" ("1" represents the offer is being called up). The Monte Carlo method is applied to generate scenarios for the uncertain components in the μVPP. To deal with computational complexity brought by large number of scenarios, this paper applies a forward selection algorithm utilized in [24] to perform scenario reduction and deliver a best possible approximation of the initial stochastic data.

In this paper, a chance-constrained two-stage stochastic formulation is utilized to devise the bidding strategy for a μVPP. In the first stage, the objective is to maximize μVPP's expected net profit by adding up its income from the DA energy-reserve market and deducting the operation cost of generators. The decision variables determined in the first stage include: 1) the energy bid/offer $P_{DA,t}^E$ submitted to the DA market; 2) the reserve bid $P_{up,t}^R/P_{dw,t}^R$ submitted to the DA market; 3) the operation schedule (ON/OFF status $o_{i,t}$, start-up decision $u_{i,t}$ and shut-down decision $v_{i,t}$) and output power $P_{i,t}^{Gen}$ for each generator; 4) the available upward/downward reserve power $r_{i,t}^{Gen,up}/r_{i,t}^{Gen,dw}$ sourced from dispatchable generator and 5) the scheduled usage $P_t^{W,S}$ of wind power based on the forecasted output.

The objective function of the first stage is formed as follows:

$$\max \ S_{DA}^R + S_{DA}^{Load} - S_{DA}^E - S_{DA}^{Gen}$$

$$= \sum_{t=1}^{NT} \left\{ C_{DA}^R \left(P_{up,t}^R + P_{dw,t}^R \right) + \omega \eta C_t^{E,DA} P_t^{L,DA} - \eta C_t^{E,DA} \right.$$

$$\left. \times P_{DA,t}^E - \sum_{i=1}^{NG} \left(C_i^{Gen} P_{i,t}^{Gen} + C_i^{SU} u_{i,t} + C_i^{SD} v_{i,t} \right) \right\} \tag{10}$$

where the DA revenue comes from submitting reserve offers S_{DA}^R and energy retail S_{DA}^{Load}. The DA cost includes expected

payment for energy bid S_{DA}^E (if the energy offer instead of bid is submitted in DA market, S_{DA}^E is another source of revenue) and operation cost S_{DA}^{Gen} of generators.

Subject to the following constraints:

$$-EXCH_{\max} \le P_{DA,t}^E \le EXCH_{\max} \tag{11}$$

$$P_i^{Gen} \le P_{i,t}^{Gen} o_{i,t} \le \bar{P}_i^{Gen} \quad \forall i, \forall t \tag{12}$$

$$-o_{i,t-1} + o_{i,t} - o_{i,k} \le 0, \quad 1 \le k - (t-1) \le T_{on}^{Gen} \\ \forall i, \forall t \tag{13}$$

$$o_{i,t-1} - o_{i,t} + o_{i,k} \le 1, \quad 1 \le k - (t-1) \le T_{off}^{Gen} \\ \forall i, \forall t \tag{14}$$

$$-o_{i,t-1} + o_{i,t} - u_{i,t} \le 0 \quad \forall i, \forall t \tag{15}$$

$$o_{i,t-1} - o_{i,t} - v_{i,t} \le 0 \quad \forall i, \forall t \tag{16}$$

$$P_{i,t}^{Gen} - P_{i,t-1}^{Gen} \le \left(2 - o_{i,t-1} - o_{i,t} \right) P_i^{Gen} \\ + \left(1 + o_{i,t-1} - o_{i,t} \right) RU_i \quad \forall i, \forall t \tag{17}$$

$$P_{i,t-1}^{Gen} - P_{i,t}^{Gen} \le \left(2 - o_{i,t-1} - o_{i,t} \right) P_i^{Gen} \\ + \left(1 - o_{i,t-1} + o_{i,t} \right) RD_i \quad \forall i, \forall t \tag{18}$$

$$0 \le P_t^{W,S} \le P_t^{W,DA} \quad \forall t \tag{19}$$

$$P_{DA,t}^E + \sum_{i=1}^{NG} P_{i,t}^{Gen} + P_t^{W,S} = P_t^{L,DA} \quad \forall i, \forall t \tag{20}$$

$$0 \le r_{i,t}^{Gen,up} \le \rho_{up} \bar{P}_i^{Gen} \quad \forall i, \forall t \tag{21}$$

$$0 \le r_{i,t}^{Gen,dw} \le \rho_{dw} \bar{P}_i^{Gen} \quad \forall i, \forall t \tag{22}$$

$$P_{i,t}^{Gen} + r_{i,t}^{Gen,up} \le \bar{P}_i^{Gen} o_{i,t} \quad \forall i, \forall t \tag{23}$$

$$P_{i,t}^{Gen} - r_{i,t}^{Gen,dw} \ge P_i^{Gen} o_{i,t} \quad \forall i, \forall t \tag{24}$$

$$P_{i,t}^{Gen} - P_{i,t-1}^{Gen} + r_{i,t}^{Gen,up} \le \left(2 - o_{i,t-1} - o_{i,t} \right) P_i^{Gen} \\ + \left(1 + o_{i,t-1} - o_{i,t} \right) RU_i \quad \forall i, \forall t \tag{25}$$

$$P_{i,t-1}^{Gen} - P_{i,t}^{Gen} + r_{i,t}^{Gen,dw} \le \left(2 - o_{i,t-1} - o_{i,t} \right) P_i^{Gen} \\ + \left(1 - o_{i,t-1} + o_{i,t} \right) RD_i \quad \forall i, \forall t \tag{26}$$

$$0 \le P_{up,t}^R \le P_t^{L,DA} \quad \forall t \tag{27}$$

$$0 \le P_{up,t}^R \le \sum_{i=1}^{NG} r_{i,t}^{Gen,up} \quad \forall i, \forall t \tag{28}$$

$$0 \le P_{dw,t}^R \le P_t^{L,DA} \quad \forall t \tag{29}$$

$$0 \le P_{dw,t}^R \le \sum_{i=1}^{NG} r_{i,t}^{Gen,dw} \quad \forall i, \forall t \tag{30}$$

$$\Pr \left\{ \sum_{i=1}^{NG} P_{i,t}^{Gen} + EXCH_{\max} + \sum_{i=1}^{NG} r_{i,t}^{Gen,up} \ge P_{s,t}^{L,RT} - P_{s,t}^{W,RT} \right\} \\ \ge 1 - \varepsilon_{LOLP} \quad \forall t \tag{31}$$

$$\Pr \left\{ \sum_{i=1}^{NG} P_{i,t}^{Gen} + P_{DA,t}^E - P_{up,t}^R + \sum_{i=1}^{NG} r_{i,t}^{Gen,up} \ge P_{s,t}^{L,RT} - P_{s,t}^{W,RT} \right\} \\ \ge 1 - \varepsilon_{LOLP} \quad \forall t \tag{32}$$

where the constants include: transaction limit $EXCH_{\max}$ (kW) between μVPP and distribution pool market; the upper limit $\bar{P}_i^{Gen}$ (kW) and the lower limit P_i^{Gen} (kW) of the ith dispatchable generator output power; the minimum time T_{on}^{Gen} (h)

that generators should be on and the minimum time T_{off}^{Gen} (h) they should be off per day; ramp up limit RU_i (kW/h) and ramp down limit RD_i (kW/h) that characterize the speed of providing upward or downward spinning reserve of the ith generator; the DA forecasted wind power $P_t^{W,DA}$ (kW) and forecasted load $P_t^{L,DA}$ (kW) during period t; the RT wind power $P_{s,t}^{W,RT}$ (kW) and RT load $P_{s,t}^{L,RT}$ (kW) in scenario s during period t; the percentage of ρ_{up}/ρ_{dw} that limits the maximum capacity of upward/downward spinning reserve with regard to generation capability; the LOLP level ε_{LOLP} and the price constants.

The objective function (10) aims at maximizing the expected DA profit of μVPP while considering the limits of its generators and guaranteeing a small probability of load loss. Constraints (11) - (32) apply in a day-ahead scheduling period of 24 hours. In Equation (11) defines the upper and lower limits of the DA energy bid/offer. Equation (12) ensures the power output of each generator is within its capacity. Equation (13) and (14) are the minimum on time and minimum off time constraints for generators respectively. Equation (15) and (16) define the start-up and shut-down variables. Equation (17) and (18) apply the ramping rate limits on the speed of each generator to increase or decrease its power output. Equation (19) represents the fact that the scheduled wind power will not exceed the forecasted value. Equation (20) is the power balance constraint between supply and demand inside μVPP. Should the DA reserve offer be called up to produce, equation (21) and (22) set the upper limit of upward and downward spinning reserve that are available from each generator. However, the production of upward or downward spinning reserve capacity should also abide by the output power limit and ramping limit as indicated by (23) - (24) and (25) - (26) respectively. Equation (27) indicates that the upward reserve capacity offered by μVPP should not exceed its demand level since satisfying the load is the priority of DER production. Equation (28) explains that the upward reserve capacity offer is originated from ramping up the generator output. Similar constraints (29) and (30) apply the same rules to the downward reserve offer. Equation (31) is the chance constraint for LOLP if upward reserve offer is not called up to produce. Equation (32) is the chance constraint for LOLP if upward reserve offer is called up to produce. In this case the power flows from the μVPP to the distribution pool and the upward reserve capacity will be deducted from the upward spinning reserves. The remainder of the power supply should guarantee a low probability of load loss.

The chance constraints (31) and (32) are converted into their equivalent deterministic formulation as follows:

$$\sum_{i=1}^{NG} P_{i,t}^{Gen} + EXCH_{max} + \sum_{i=1}^{NG} r_{i,t}^{Gen,up}$$
$$\geq E\left(P_{s,t}^{L,RT} - P_{s,t}^{W,RT}\right) + \phi^{-1}\left(1 - \varepsilon_{LOLP}\right)$$
$$\times \sigma\left(P_{s,t}^{L,RT} - P_{s,t}^{W,RT}\right) \quad \forall s, \forall t \quad (33)$$

$$\sum_{i=1}^{NG} P_{i,t}^{Gen} + P_{DA,t}^E - P_{up,t}^R + \sum_{i=1}^{NG} r_{i,t}^{Gen,up}$$
$$\geq E\left(P_{s,t}^{L,RT} - P_{s,t}^{W,RT}\right) + \phi^{-1}\left(1 - \varepsilon_{LOLP}\right)$$
$$\times \sigma\left(P_{s,t}^{L,RT} - P_{s,t}^{W,RT}\right) \quad \forall s, \forall t \quad (34)$$

where the mean of the RT net load (i.e. net load is obtained by deducing the wind power from load) is calculated as

$$E\left(P_{s,t}^{L,RT} - P_{s,t}^{W,RT}\right) = P_t^{L,DA} - P_t^{W,DA} \quad \forall t. \quad (35)$$

And the standard deviation of the stochastic net load is calculated as

$$\sigma\left(P_{s,t}^{L,RT} - P_{s,t}^{W,RT}\right)$$
$$= \sqrt{\pi_s^* \sum_{s=1}^{NS}\left(P_{s,t}^{L,RT} - P_{s,t}^{W,RT} - E\left(P_{s,t}^{L,RT} - P_{s,t}^{W,RT}\right)\right)^2}.$$
$$\forall t. \quad (36)$$

Also, the component $\phi^{-1}\left(1 - \varepsilon_{LOLP}\right)$ in the deterministic equivalence computes the inverse of the normal cumulative distribution function with the probability $1 - \varepsilon_{LOLP}$, mean 0 and standard deviation 1. The conversion of chance constraints into their deterministic form is shown in the appendix.

In the second stage, the objective is to maximize the gains (or minimize the losses) of μVPP profit brought by RT uncertainties. The second stage objective function is presented in equation (37)

$$\max S_{RT}^R + S_{RT}^{Load} - S_{RT}^E - S_{RT}^{Gen} - S_{RT}^{Loss}$$
$$= \sum_{s=1}^{NS} \sum_{t=1}^{NT} \left\{ \pi_s^* \left\{ C_{RT}^R \left(P_{up,t}^R SIG_{s,t}^{up} + P_{dw,t}^R SIG_{s,t}^{dw}\right) \right. \right.$$
$$+ \omega \eta C_{s,t}^{E,RT} \left(P_{s,t}^{L,RT} - P_t^{L,DA}\right)$$
$$- \eta C_{s,t}^{E,RT} \left(\Delta P_{s,t}^{E+} - \Delta P_{s,t}^{E-}\right)$$
$$- \eta \left(C_{s,t}^{E,RT} - C_t^{E,DA}\right) P_{DA,t}^E$$
$$\left. \left. - \sum_{i=1}^{NG} C_i^{Gen} \Delta P_{s,i,t}^{Gen} - C_{loss} P_{s,t}^{Loss} \right\} \right\}. \quad (37)$$

Subject to the following constraints:

$$-r_{i,t}^{Gen,dw} \leq \Delta P_{s,i,t}^{Gen} \leq r_{i,t}^{Gen,up} \quad \forall s, \forall i, \forall t \quad (38)$$

$$0 \leq \Delta P_{s,t}^{E+} \leq EXCH_{max},$$
$$0 \leq \Delta P_{s,t}^{E-} \leq EXCH_{max} \quad \forall s, \forall t \quad (39)$$

$$-EXCH_{max} \leq P_{DA,t}^E + \Delta P_{s,t}^{E+} - \Delta P_{s,t}^{E-} \leq EXCH_{max}$$
$$\forall s, \forall t \quad (40)$$

$$0 \leq P_{s,t}^{W,A} \leq P_{s,t}^{W,RT} \quad \forall s, \forall t \quad (41)$$

$$0 \leq P_{s,t}^{Loss} \leq \zeta P_{s,t}^{L,RT} \quad \forall s, \forall t \quad (42)$$

$$\left(P_{DA,t}^E + \Delta P_{s,t}^{E+} - \Delta P_{s,t}^{E-}\right) + \sum_{i=1}^{NG}\left(P_{i,t}^{Gen} + \Delta P_{s,i,t}^{Gen}\right) + P_{s,t}^{W,A}$$
$$= P_{s,t}^{L,RT} - P_{s,t}^{Loss} \quad \forall s, \forall t \quad (43)$$

$$-P_{up,t}^R SIG_{s,t}^{up} + P_{dw,t}^R SIG_{s,t}^{dw}$$
$$= \Delta P_{s,t}^{E+} - \Delta P_{s,t}^{E-} \quad \forall s, \forall t. \tag{44}$$

The second stage objective function (37) aims at maximizing the increment (or equally minimizing the decrement) of expected μVPP profit in different scenarios with specified probability. The first term represents the RT income S_{RT}^R from delivering the offered reserve capacity. The second term refers to the income variation S_{RT}^{Load} caused by uncertain RT load. The third and fourth terms of equation (37) stand for cost variation S_{RT}^E which settles the RT payment for any upward or downward changes to energy bid and for the price difference between the DA market and the RT market. The fifth term is the cost variation S_{RT}^{Gen} for the increment or decrement in output power for all generators. The last term $C_{loss}P_{s,t}^{Loss}$ is the compensation cost S_{RT}^{Loss} to end-users for possible load loss in certain scenarios. The first stage decision variables $P_{DA,t}^E$, $P_{up,t}^R$, $P_{dw,t}^R$, $P_{i,t}^{Gen}$, $r_{i,t}^{Gen,up}$ and $r_{i,t}^{Gen,dw}$ are still involved in the second stage formulation. Additional decision variables include: 1) the upward change $\Delta P_{s,t}^{E+}$ (kW) or downward change $\Delta P_{s,t}^{E-}$ (kW) to the DA energy bid/offer in scenario s during period t; 2) the change to the ith scheduled generator output power $\Delta P_{s,i,t}^{Gen}$ (kW) in scenario s during period t; 3) the actual wind power usage $P_{s,t}^{W,A}$ (kW) in scenario s during period t according to the RT wind power production and 4) the load loss $P_{s,t}^{Loss}$ (kW) in scenario s during period t. Additional constants include: probability π_s^* of selected scenarios; call up signals $SIG_{s,t}^{up}/SIG_{s,t}^{dw}$ for reserve offers in scenario s during period t and the constant ζ that represents the maximum percentage of load loss that is tolerable for end-users.

As for constraints, (38) - (44) still apply in the DA scheduling period although they define the RT variables. Equation (38) ensures that the adjustment to the generator output lies within the limits of upward/downward spinning reserve. Equation (39) and (40) address that the transaction limit should not be exceeded when changing the energy bid/offer capacity in RT market. Equation (41) represents the constraint for actual wind power usage in different scenarios. The chance constraints (31) - (32) guarantee a low probability of load loss event, however, the capacity of load loss should be confined to a small portion ζ of load as equation (42) indicates. Equation (43) is the RT power balance constraint between supply and demand for the μVPP. Finally, the power flow relationship at the distribution network connection point is described in an equality constraint (44).

To sum up, the two-stage stochastic bidding strategy is formulated as a mixed-integer linear programming (MILP) problem with the first stage objective (10) subjected to the first stage constraints (11) - (32) and the second stage objective (37) subjected to the second stage constraints (38) - (44). The two-stage problem aims at deriving a well-informed day-ahead operation schedule with estimated real-time realization of uncertain components. It is solved concurrently with state-of-the-art solvers such as CPLEX.

IV. COMPARATIVE PERFORMANCE STUDY

In the comparative performance study, the interrelation between μVPP design and its projected profit is addressed. Two parametric indexes are introduced: the DER index that represents the ratio of on-site DER capacity over the value of maximum load level and the Renewable Energy Source (RES) index that is defined as the ratio of RES capacity over the total DER capacity. The first case is set up with fixed uncertainty level for volatile parameters, where μVPPs with different DER indexes and RES indexes are studied. The second case studies the impact of wind power uncertainty, load uncertainty and LOLP level individually. The third case compares the proposed chance-constrained formulation with the classical Monte Carlo RT recourse approach. The fourth case analyzes the impact of the congestion on the μVPP bidding behaviors. Considering the decarbonization strategy promoted by the UK government, the last case investigate the impact on μVPPs' profit brought by the introduction of carbon tax.

The UK DA forecasted retail electricity price is extracted from Nord Pool price data 2016 [25], while the carbon tax rates are calculated according to the UK government's policy on carbon pricing [26]. The μVPP candidate, a residential community located in West Midlands County, has around 200 households with an average of 533kW daily consumption power. End-users of the community are subject to a 10% discount on retail price and 200% compensation for load loss. To provide guidance to deploy DERs in this community, different sizes of dispatchable generators from 165kW to 660kW and wind turbines from 20kW to 660kW are studied. All case studies are coded with YALMIP and CPLEX 12.1.4 is utilized as the solver. The program runs on an Intel Core-i5 2.5-GHz computer and the run time for the algorithm is around 80 seconds.

A. IMPACT OF DER INDEX AND RES INDEX
In this case, four DER indexes of 1/4, 1/2, 3/4 and 1 are studied. Nine RES indexes from 0 to 1 with a gradient of 1/8 are also introduced. Firstly, the bidding behavior in DA energy-reserve market for different combinations of DER index (I1) and RES index (I2) is depicted in Fig. 3.

The diagram on the left-hand side of Fig. 3(a) shows a similar pattern of bidding behavior for μVPPs with the same RES index and different DER index: the peak and valley bidding curves overlap with peak and valley load. When the DER capacity is large enough, the μVPP can make energy offers to the pool during low demand period of 3-4 a.m. and 6-7 a.m. The diagram on the right-hand side of Fig. 3(a) demonstrates how the RES index impacts the bidding behavior under a fixed DER capacity: with a low RES penetration level of 0 and 1/4 Index value, the μVPP is more inclined to an autonomy state from the grid and will only make energy bid during energy intensive period of the day. The capacity of the bid is also lower with low RES indexes since dispatchable generators, which account for the larger half of
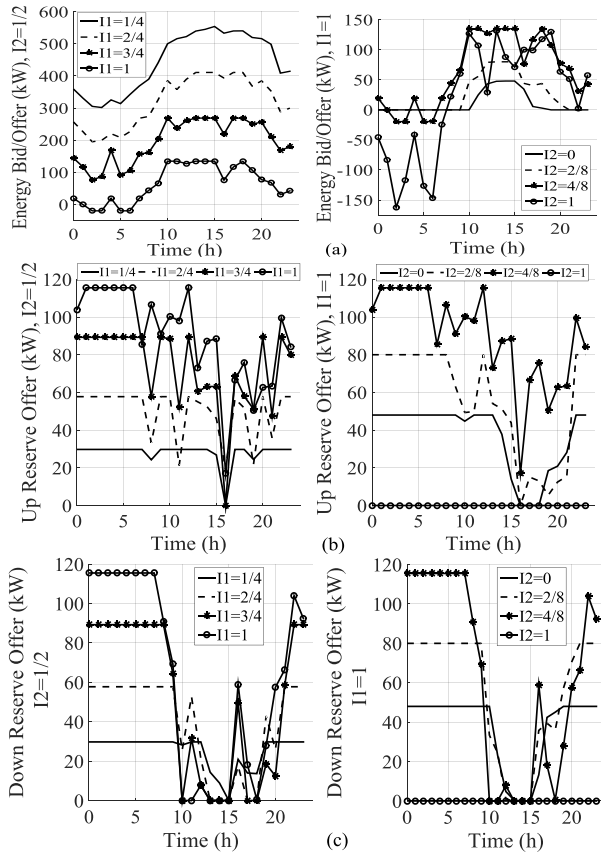
FIGURE 3. μVPP bidding behaviors: (a) energy market bidding; (b) upward reserve offering; (c) downward reserve offering.

FIGURE 4. μVPP profit for different DER and RES indexes.

the DER, can provide more upward spinning reserve to be used inside the μVPP. For higher RES index of 1/2 and 1, the bidding/offering pattern becomes more volatile. Such a volatile bidding/offering behavior leads to heavy reliance on the utility grid, which increases μVPP's vulnerability to fault events.

In the left diagram of Fig. 3(b), the upward reserve offers submitted by μVPPs with different DER indexes share the same pattern. Intuitively, a larger DER capacity means a higher offer capacity from dispatchable generators. When the DER is made up entirely of wind generation, μVPP becomes incapable of providing upward reserve offer.

The provision of downward reserve offer as indicated in Fig. 3(c) shares similarities with upward reserve offering except for the energy intensive period of 10 a.m. to 18 p.m., when the μVPP rarely submits downward reserve offers. This is because the submission of downward reserve offers during the high demand period is only driven by lower energy price. If the cost of dispatchable generation is lower than the RT energy price, μVPP will not provide downward reserve service for economic concerns.

Secondly in Case A, the daily profit of the μVPP in terms of DER index and RES index is presented in Fig. 4.

The profit of μVPP increases with a rising DER index and RES index, this is due to the assumption that wind
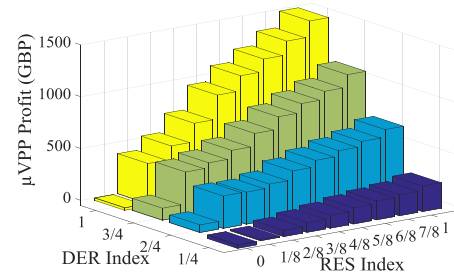
turbine has zero operation cost which is an optimistic setup compared with practice. However, the μVPP business model has incorporated a pricing mechanism to improve the fairness to different DER allocations: for those μVPPs with high RES penetration (i.e. marked by a RES index that is close to or equal to 100%), the transaction limit $EXCH_{max}$ between the μVPP and the main grid is also high to guarantee that μVPP could always import from the main grid when underproduction occurs in real-time. Based on the μVPP-DSO agreement described in Section II, a higher transaction limit corresponds to more expensive tariff for energy import. As shown in the right diagram of Fig. 3(a), μVPP with high RES index has more frequent and larger purchases in the energy market to make up for the shortage caused by wind production uncertainty. Another reason for the high projected profit earned by RES-dominated μVPP is that the energy offers from the large wind generation are assumed to be accepted by the pool market completely. Additionally, high penetration of RES requires major initial investment followed by regular expenses on maintenance and repair. A μVPP with a seemingly high daily profit could also risk being put on a slow lane to recoup its capital investment. To sum up, Fig. 4 is produced under an optimistic market setup with pricing measure to increase the credibility of the result. It provides a reference baseline to observe the effect of altering the DER allocation on the projected μVPP profit.

B. IMPACT OF UNCERTAINTIES AND LOLP
In this case, the impact of narrowing down the parameter uncertainties of wind power and load is demonstrated in Fig. 5. It is pointed out that extra revenue can be generated by acquiring more accurate forecast information during DA bidding stage. Fig. 5(a) shows how much extra revenue can be obtained by narrowing down the wind forecast error from 20% to 0. The revenue rises with an increasing capacity of DER and the increasing share of RES, but the additional income barely achieves 5% increase in percentage terms for all possible configurations. Therefore, a small level of wind power forecast error is tolerable for μVPPs but an accurate forecast system will be beneficial to those with large wind turbine assets. Fig. 5(b) displays the extra revenue generated by slashing the load forecast error from 5% to 0. Unlike wind power uncertainty, an accurate load forecast information proves to be crucial for μVPPs with all configurations.
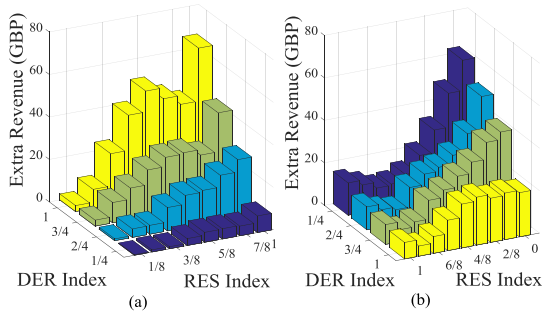
FIGURE 5. Extra revenue obtained by (a) eliminating 20% wind forecast error and (b) eliminating 5% load forecast error.

The maximum profit increments in percentage terms are 71.28%, 36.88% and 86.66% for μVPP with DER index 1/2, 3/4 and 1 respectively. For the μVPP with DER index 1/4, the forecast error reduction of load could even recover a losing business back to a break-even point. To sum up, accurate load forecast system is mandatory for profit-motivated μVPPs, especially for those with small wind turbine assets because a more volatile load would cost more energy bidding variations and more spinning reserves to be consumed inside the μVPP.

The second result presented in this case is the impact of LOLP level on the profit and upward reserve offering behavior. The European Parliament has issued a regulation on risk-preparedness in the electricity sector, in which the security of power supply requires that 95% to 99% of the time no one should be involuntarily disconnected. Consequently, the value of LOLP could be set as 0.01, 0.02 and 0.05. The result of an example μVPP with DER index 1/4 is given in Table 1.

TABLE 1. Impact of LOLP on profit and upward reserve offering for DER index 1/4.

Result \ I2	$P_{up,t}^R$ kW 0.01	$P_{up,t}^R$ kW 0.02	$P_{up,t}^R$ kW 0.05	$\Delta P_{up,t}^R$ (%) (0.01 → 0.02)	$\Delta P_{up,t}^R$ (%) (0.01 → 0.05)	ΔS_{uVPP} (%) (0.01 → 0.05)
0	290.37	415.04	602.03	42.93% ↑	107.33% ↑	36.86% ↑
1/8	404.69	532.68	723.01	31.63% ↑	78.66% ↑	186.11% ↑
2/8	581.77	638.54	788.39	9.76% ↑	35.52% ↑	38.60% ↑
3/8	627.97	697.67	782.41	11.10% ↑	24.59% ↑	18.38% ↑
4/8	607.25	649.63	674.00	6.98% ↑	10.99% ↑	9.63% ↑
5/8	509.23	517.89	520.85	1.70% ↑	2.28% ↑	6.17% ↑
6/8	358.75	362.92	372.21	1.16% ↑	3.75% ↑	4.58% ↑
7/8	192.50	192.50	192.50	0	0	3.66% ↑
1	0	0	0	0	0	3.33% ↑

Four specific configurations are worth highlighting: for μVPPs with extremely high share of dispatchable generators in their energy mix (represented by low RES index 0 and 1/8), the LOLP setting has a tremendous impact on the upward reserve offer behavior and a LOLP relaxation from 0.01 to 0.05 could potentially recover a losing μVPP operation to the break-even point. To achieve the tradeoff between supply security (guaranteed by low LOLP) and eco-

nomic viability (financially sound under higher LOLP), these μVPPs with low RES index should consider the deployment of controllable load to actively shed the lost load. On the other hand, some μVPPs have extremely low capacity of dispatchable generators (represented by high RES index 7/8 and 1) and the upward spinning reserve is not enough to be submitted as reserve offers. Thus, it is not necessary for these μVPPs to participate in the reserve market. Also, the insignificant rise in extra revenue makes them less motivated to secure low LOLP.

C. COMPARISON OF RISK-HEDGING METHODS

To address the competitiveness of the proposed chance-constrained formulation, a reference case is derived by solving a deterministic DA problem and applying the Monte Carlo recourse method in the RT stage to obtain the best approximation of μVPP profit. The DA objective (10) subjected to constraints (11) - (30) is solved independently as a deterministic problem, with chance constraints (31) - (32) replaced by the following limits (45) - (46):

$$-EXCH_{\max} \leq P_{DA,t}^E - P_{up,t}^R \leq EXCH_{\max} \quad \forall t \quad (45)$$

$$-EXCH_{\max} \leq P_{DA,t}^E + P_{dw,t}^R \leq EXCH_{\max} \quad \forall t \quad (46)$$

where the provision of upward and downward reserve strictly obeys the transaction limit at the grid connection point, regardless of any RT stochastic parameters. Then the already derived bid/offer capacities and the dispatchable generation schedule are utilized in the RT recourse with objective (37) subjected to constraints (38) - (44). Both risk-hedging methods are applied in an example μVPP with DER index 1 and RES index 1/2. The result is displayed in Table 2.

TABLE 2. Comparison between two risk-hedging methods in μVPP bidding strategy.

Methods \ Results	Chance-Constrained	Deterministic & Monte Carlo Recourse
Total Energy bid/offer (kW)	1547.11	960.09
Total Up reserve offer (kW)	2161.95	1889.46
Total Down reserve offer (kW)	1517.59	1582.29
Loss of Load Probability	5%	69%
Total energy payment in DA and RT market (£)	125.44	109.80
Total reserve income in DA and RT market (£)	202.00	178.56
Avg. Load Loss Penalty (£)	0.05	5.13
μVPP Profit (£)	926.15	900.94
Computation time (s)	80.1	104.0

Based entirely from DA forecasted knowledge, the deterministic formulation requires the forecasted load to be satisfied without any tolerance to loss, thus the μVPP becomes more conservative in terms of providing upward reserve services. Although the RT recourse has made every effort to accommodate the uncertainties and achieved 97.3% of the proposed profit, it still yields a staggering 69% probability of

load loss event and a daily penalty that is more than 100 times of the proposed method. On the other hand, the proposed method excels in terms of accurate control of load loss, higher daily profit and computational efficiency.

D. RIVAL's IMPACT ON BIDDING BEHAVIORS

The bidding behavior of the μVPP is influenced by rivals located at its nearby buses. For price-taking μVPPs, such impact takes place in the event of distribution line congestion when the feeders are heavily loaded. A three bus DC network model is utilized in this case and presented in Fig. 6: two rival μVPPs are represented by two adjacent nodes (node 1 and node 2) while node 3 is the energy-reserve pool managed by the DSO.
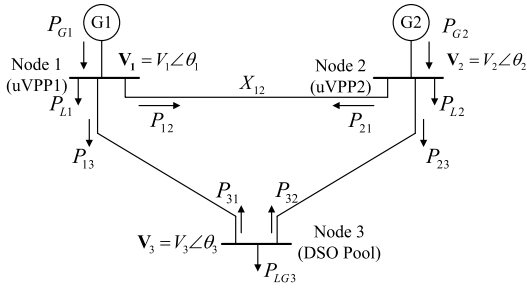

FIGURE 6. Three bus DC network model for μVPPs.

With the following additional constraints of the DC power flow model added to the optimization problem:

$$P_{G1} - P_{L1} - \left(\frac{1}{X_{12}} + \frac{1}{X_{13}}\right)\theta_1 + \frac{1}{X_{12}}\theta_2 + \frac{1}{X_{13}}\theta_3 = 0 \tag{47}$$

$$P_{G2} - P_{L2} - \left(\frac{1}{X_{12}} + \frac{1}{X_{23}}\right)\theta_2 + \frac{1}{X_{12}}\theta_1 + \frac{1}{X_{23}}\theta_3 = 0 \tag{48}$$

$$0 - P_{LG3} - \left(\frac{1}{X_{13}} + \frac{1}{X_{23}}\right)\theta_3 + \frac{1}{X_{13}}\theta_1 + \frac{1}{X_{23}}\theta_2 = 0 \tag{49}$$

where the parameter P_{LG3} represents the net load or the net surplus of the pool market.

And the following additional constraints of the line limits are added to the optimization problem:

$$-P_{12}^{\max} \leq P_{12} \leq P_{12}^{\max} \tag{50}$$

$$-P_{13}^{\max} \leq P_{13} \leq P_{13}^{\max} \tag{51}$$

$$-P_{23}^{\max} \leq P_{23} \leq P_{23}^{\max}. \tag{52}$$

And the constraints for state variables are added to the optimization problem

$$0 \leq \theta_1 \leq 0 \tag{53}$$

$$-\infty \leq \theta_2 \leq \infty \tag{54}$$

$$-\infty \leq \theta_3 \leq \infty. \tag{55}$$

If network congestion is not considered, the bidding quantity of individual μVPPs in the energy market is limited only

by the overall transaction limit. However, the distribution line 1-3 between node 1 and node 3 is congested during peak load period since the power flow requested by the μVPP exceeds the thermal limit. As shown in Fig. 7(a), the energy bidding trajectory becomes flat with congestion considered.
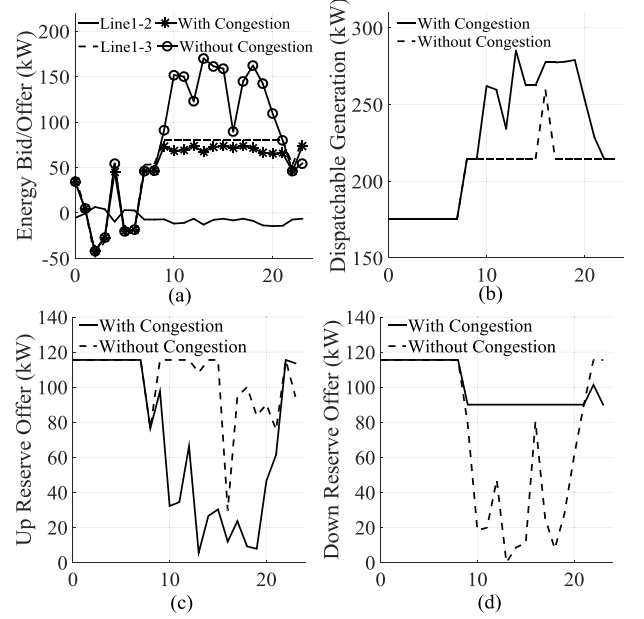

FIGURE 7. Impact on behaviors: (a) energy market bidding; (b) dispatchable generation; (c) upward reserve offering; (d) downward reserve offering.

To satisfy the demand within μVPP that has congestion, the dispatchable generators must ramp up and produce more power as Fig. 7(b) indicates. Consequently, Fig. 7(c) and Fig. 7(d) show the decreased ability to provide upward reserve offer and the increased ability to provide downward reserve offer.

E. IMPACT OF IMPLEMENTING CARBON TAX

To promote the decarbonization of electricity supply and reduce greenhouse gas emissions, the UK government has introduced a carbon tax levied on the electricity produced by generators using fossil fuels. The carbon tax ranges from 1.3p/kWh to 3.9p/kWh and it will be added to the variable unit cost for the dispatchable generators in the original two-stage μVPP bidding formulation presented in Section III. This case investigates how μVPPs, with their different shares of dispatchable generators, are affected by the implementation of carbon tax in terms of economic profit.

In Fig. 8, the blue bar represents μVPPs' profit without the consideration of carbon tax, where the variable unit cost is the actual production cost of dispatchable generators. The green bar and yellow bar depict μVPPs' profits with a low carbon tax rate of 1.3p/kWh and a high rate of 3.9p/kWh respectively. The introduction of carbon tax decreases μVPPs' profit due to an increased operation cost of dispatchable generators and the reduction grows more significant with a higher tax rate. For those μVPPs with extremely high share of dispatchable
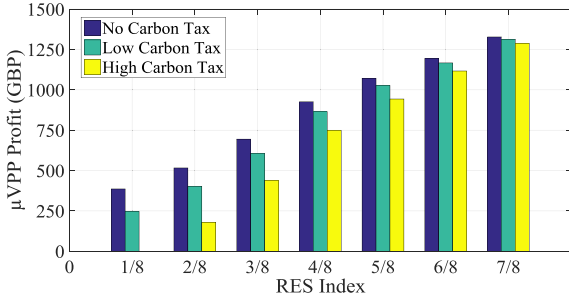
FIGURE 8. Impact of carbon tax on ṭVPPs with different RES indexes.

generators (characterized by low RES index of 1/8), the profit even drops to zero in the presence of a high carbon tax rate. Secondly, with the RES index increases from 1/8 to 7/8, the electricity supply of the μVPP becomes more decarbonized and the reduction on profit brought by carbon tax becomes less obvious. With the implementation of carbon tax, higher penetration of RES is recommended for μVPP investors.

V. CONCLUSION

This paper describes the bidding strategy formulation for price-taking micro Virtual Power Plants (μVPPs) to gain competitive advantage in the upcoming deployment of the distribution system pool. Beside active bidding and offering in the energy pool, the μVPP also has its asset value stretched to provide ancillary services. In a foreseeable future, the energy-reserve equilibrium will be achieved locally by the interworking of multiple μVPPs. The decreasing investment for distribution network expansion and the increasing revenue for μVPPs will encourage the newborn distribution system pool to become a highly competitive market. End-users will have a greater choice of energy suppliers which may yield retail electricity price reductions. μVPPs, recognized as full-dependent, semi-autonomous and full-autonomous in terms of DER coverage and full-dispatchable, semi-renewable and full-renewable in terms of RES share, are shown to have significant differences in bidding behaviors and projected daily profit. Also the results have demonstrated how μVPP owners are affected by the implementation of carbon tax.

The numerical tests have shown that accurate wind power and load forecasting bring additional revenue to the μVPP. The extra income can also be obtained by relaxing the required LOLP level but a compromise must be made financially to guarantee the level of the security of supply. As a computationally efficient and technically secure method, the proposed chance-constrained two-stage μVPP optimization provides valuable guidance to investors in the determination of DER and RES capacities and the mitigation of risks brought by uncertainties. The deployment of such μVPPs in the distribution network is a potential solution to better integrate DERs into the existing networks without inflicting high retrofit cost.

Further improvement on the μVPP profit and supply adequacy could be achieved by introducing demand response program in the form of contractual commitment with end-users. By installing controllable loads, the load power could be adjusted or shed when the "Loss of Load" scenario arises again. Consequently, μVPP could avoid paying high penalty for the load loss and free more capacity of the dispatchable generators to be consumed inside the μVPP or offered to the pool market. Part of the newly generated revenue stream could be used to reward and motivate the participating end-users.

APPENDIX
DETERMINISTIC EQUIVALENCE OF CHANCE CONSTRAINTS (31) – (32)

The general form of chance constraint is presented as follows:

$$\Pr\{h(x) \geq \xi\} \geq \alpha \tag{56}$$

where x is the decision variable, ξ is a random coefficient whose value subjects to stable distribution and α is the confidence level which means the probability of the value of $h(x)$ being higher than or equal to ξ should be at least α. The conversion of chance constraint to its deterministic equivalence consists of two steps: firstly, the inequality $h(x) \geq \xi$ is transformed into $h'(x) \geq \xi'$ where ξ' subjects to standard normal distribution; then the deterministic equivalence of (56) is derived as

$$h'(x) \geq \phi^{-1}(\alpha) \tag{57}$$

where $\phi^{-1}(\alpha)$ computes the inverse of normal cumulative distribution function with probability α, mean 0 and standard deviation of 1.

The chance constraint (31) is reformulated in its general form and its terms are denoted as

$$h(x) = \sum_{i=1}^{NG} P_{i,t}^{Gen} + EXCH_{\max} + \sum_{i=1}^{NG} r_{i,t}^{Gen,up}$$
$$\xi = P_{s,t}^{L,RT} - P_{s,t}^{W,RT}$$
$$\alpha = 1 - \varepsilon_{LOLP}. \tag{58}$$

By carrying out the first step of the conversion, the updated terms are derived in (59)

$$h'(x)$$
$$= \frac{\left(\sum_{i=1}^{NG} P_{i,t}^{Gen} + EXCH_{\max} + \sum_{i=1}^{NG} r_{i,t}^{Gen,up}\right) - E\left(P_{s,t}^{L,RT} - P_{s,t}^{W,RT}\right)}{\sigma\left(P_{s,t}^{L,RT} - P_{s,t}^{W,RT}\right)}$$
$$\xi' = \frac{\left(P_{s,t}^{L,RT} - P_{s,t}^{W,RT}\right) - E\left(P_{s,t}^{L,RT} - P_{s,t}^{W,RT}\right)}{\sigma\left(P_{s,t}^{L,RT} - P_{s,t}^{W,RT}\right)}. \tag{59}$$

Therefore, the deterministic equivalence of the chance constraint (31) is derived as (33) shows. And the same procedure

applies for chance constraint (32)

$$\frac{\left(\sum_{i=1}^{NG} P_{i,t}^{Gen} + EXCH_{\max} + \sum_{i=1}^{NG} r_{i,t}^{Gen,up}\right) - E\left(P_{s,t}^{L,RT} - P_{s,t}^{W,RT}\right)}{\sigma\left(P_{s,t}^{L,RT} - P_{s,t}^{W,RT}\right)}$$
$$\geq \phi^{-1}\left(1 - \varepsilon_{LOLP}\right).$$

REFERENCES

[1] Ofgem. *RIIO—A New Way to Regulate Energy Networks.* Accessed on: Jul. 22, 2016. [Online]. Available: https://www.ofgem.gov.uk/ofgem-publications/76341/riio-oct-press-notice.pdf

[2] Imperial College London. *Understanding the Balancing Challenge.* Accessed on: Jul. 1, 2016. [Online]. Available: https://www.gov.uk/government/uploads/system/uploads/attachment_data/file/48553/5767-understanding-the-balancing-challenge.pdf

[3] A. J. Conejo, J. M. Morales, and J. A. Martinez, "Tools for the analysis and design of distributed resources—Part III: Market studies," *IEEE Trans. Power Del.*, vol. 26, no. 3, pp. 1663–1670, Jul. 2011.

[4] F. Farzan, S. Lahiri, M. Kleinberg, K. Gharieh, F. Farzan, and M. Jafari, "Microgrids for fun and profit: The economics of installation investments and operations," *IEEE Power Energy Mag.*, vol. 11, no. 4, pp. 52–58, Jul./Aug. 2013.

[5] I. G. Sardou, M. E. Khodayar, K. Khaledian, M. Soleimani-Damaneh, and M. T. Ameli, "Energy and reserve market clearing with microgrid aggregators," *IEEE Trans. Smart Grid*, vol. 7, no. 6, pp. 2703–2712, Nov. 2015.

[6] I. C. Paschalidis, B. Li, and M. C. Caramanis, "Demand-side management for regulation service provisioning through internal pricing," *IEEE Trans. Power Syst.*, vol. 27, no. 3, pp. 1531–1539, Aug. 2012.

[7] E. Mashhour and S. M. Moghaddas-Tafreshi, "Bidding strategy of virtual power plant for participating in energy and spinning reserve markets—Part I: Problem formulation," *IEEE Trans. Power Syst.*, vol. 26, no. 2, pp. 949–956, May 2011.

[8] A. Chaouachi, R. M. Kamel, R. Andoulsi, and K. Nagasaka, "Multiobjective intelligent energy management for a microgrid," *IEEE Trans. Ind. Electron.*, vol. 60, no. 4, pp. 1688–1699, Apr. 2013.

[9] W. Su, J. Wang, and J. Roh, "Stochastic energy scheduling in microgrids with intermittent renewable energy resources," *IEEE Trans. Smart Grid*, vol. 5, no. 4, pp. 1876–1883, Jul. 2014.

[10] Z. Bao *et al.*, "A multi time-scale and multi energy-type coordinated microgrid scheduling solution—Part I: Model and methodology," *IEEE Trans. Power Syst.*, vol. 30, no. 5, pp. 2257–2266, Sep. 2015.

[11] E. G. Kardakos, C. K. Simoglou, and A. G. Bakirtzis, "Optimal offering strategy of a virtual power plant: A stochastic bi-level approach," *IEEE Trans. Smart Grid*, vol. 7, no. 2, pp. 794–806, Mar. 2016.

[12] J. Shen *et al.*, "A microgrid energy management system and risk management under an electricity market environment," *IEEE Access*, vol. 4, pp. 2349–2356, 2016.

[13] S. Khan, W. Gawlik, and P. Palensky, "Reserve capability assessment considering correlated uncertainty in microgrid," *IEEE Trans. Sustain. Energy*, vol. 7, no. 2, pp. 637–646, Apr. 2016.

[14] G. Liu, Y. Xu, and K. Tomsovic, "Bidding strategy for microgrid in day-ahead market based on hybrid stochastic/robust optimization," *IEEE Trans. Smart Grid*, vol. 7, no. 1, pp. 227–237, Jan. 2016.

[15] A. Khodaei, S. Bahramirad, and M. Shahidehpour, "Microgrid planning under uncertainty," *IEEE Trans. Power Syst.*, vol. 30, no. 5, pp. 2417–2425, Sep. 2015.

[16] A. Khodaei, "Resiliency-oriented microgrid optimal scheduling," *IEEE Trans. Smart Grid*, vol. 5, no. 4, pp. 1584–1591, Jul. 2014.

[17] Q. Wang, J. Wang, and Y. Guan, "Stochastic unit commitment with uncertain demand response," *IEEE Trans. Power Syst.*, vol. 28, no. 1, pp. 562–563, Feb. 2013.

[18] H. Wu *et al.*, "Chance-constrained day-ahead scheduling in stochastic power system operation," *IEEE Trans. Power Syst.*, vol. 29, no. 4, pp. 1583–1591, Jul. 2014.

[19] M. Lubin, Y. Dvorkin, and S. Backhaus, "A robust approach to chance constrained optimal power flow with renewable generation," *IEEE Trans. Power Syst.*, vol. 31, no. 5, pp. 3840–3849, Sep. 2015.

[20] F. Qiu and J. Wang, "Chance-constrained transmission switching with guaranteed wind power utilization," *IEEE Trans. Power Syst.*, vol. 30, no. 3, pp. 1270–1278, May 2015.

[21] Z. Wu, P. Zeng, X.-P. Zhang, and Q. Zhou, "A solution to the chance-constrained two-stage stochastic program for unit commitment with wind energy integration," *IEEE Trans. Power Syst.*, vol. 31, no. 6, pp. 4185–4196, Nov. 2015.

[22] Ofgem. *Electricity Distribution Structure of Charges: The Common Distribution Charging Methodology at Lower Voltages.* Accessed on: Jul. 4, 2016. [Online]. Available: https://www.ofgem.gov.uk/ofgem-publications/44179/cdcm-decision-doc-201109-2.pdf

[23] *Integration of Renewable Resources: Technical Appendices for California ISO Renewable Integration Studie.* Accessed on: Jul. 27, 2016. [Online]. Available: http://www.caiso.com/1ca5/1ca5a7a026270.pdf

[24] T. Wu, Q. Yang, Z. Bao, and W. Yan, "Coordinated energy dispatching in microgrid with wind power generation and plug-in electric vehicles," *IEEE Trans. Smart Grid*, vol. 4, no. 3, pp. 1453–1463, Sep. 2013.

[25] *Nord Pool Market Data.* Accessed on: May 20, 2016. [Online]. Available: http://www.nordpoolspot.com/Market-data1/N2EX/Auction-prices/UK/Hourly/?view=table

[26] Department of Energy & Climate Change. *Carbon Prices and Sensitivities 2010–2100 for Appraisal.* Accessed on: Jan. 25, 2017. [Online]. Available: https://www.gov.uk/government/uploads/system/uploads/attachment_data/file/483282/Data_tables_1-20_supporting_the_toolkit_and_the_guidance.xlsx

HAO FU received the B.Eng. degree in electrical and electronic engineering from the Huazhong University of Science and Technology, Wuhan, China, in 2013, the B.Eng. degree from the Department of Electronic, Electrical and Systems Engineering, University of Birmingham, Birmingham, U.K., in 2013, and the Ph.D. degree in electrical engineering from the University of Birmingham, Birmingham, U.K., in 2017. He is currently with the Central Southern China Electric Power Design Institute, Wuhan, China. His research interests are the operations in market-oriented virtual power plants.

ZHI WU received the B.Eng. and M.Sc. degrees in electrical engineering from Southeast University, Nanjing, China, in 2009 and 2012, respectively, and the Ph.D. degree from the Department of Electronic, Electrical, and Systems Engineering, University of Birmingham, Birmingham, U.K., in 2016. He is currently a Lecturer with Southeast University. His research interests include smart grid energy management systems and optimization techniques.

XIAO-PING ZHANG (M'95–SM'06) received the B.Eng., M.Sc., and Ph.D. degrees in electrical engineering from Southeast University, Nanjing, China in 1988, 1990, and 1993, respectively. He was an Associate Professor with the University of Warwick, England, U.K. He is currently a Professor of Electrical Power Systems with the University of Birmingham, Birmingham, U.K. He is also the Director of Smart Grid, Birmingham Energy Institute, Birmingham, U.K., and the Co-Director of the Birmingham Energy Storage Centre, Birmingham, U.K. From 1998 to 1999, he was visiting the University of Manchester Institute of Science and Technology, Manchester, U.K. From 1999 to 2000, he was an Alexander-von-Humboldt Research Fellow with the University of Dortmund, Dortmund, Germany. He was with the China State Grid EPRI (NARI Group) on EMS/DMS advanced application software research and development between 1993 and 1998. He coauthored the 1st and 2nd edition of the monograph *Flexible AC Transmission Systems: Modeling and Control*, (Springer, 2006 and 2012, respectively). He coauthored the book *Restructured Electric Power Systems: Analysis of Electricity Markets with Equilibrium Models*, (IEEE Press/Wiley, 2010). He pioneered the concept of global power and energy internet, energy union, and U.K. energy valley.

JOACHIM BRANDT received the Ph.D. degree from Coventry University, Coventry, U.K., in 2003. He is currently a New Technologies Consultant with E.ON, Nottingham, U.K. He specializes in the integration of renewable generation, electrification of transport, and energy storage to deliver reliable customer centric digital energy services and system flexibility of an increasingly distributed decarbonized energy supply.